Mansoura Engineering Journal

Volume 25 | Issue 3 Article 8

2-5-2021

Influence of Elevated Temperature on Fracture Behavior of Stainless Steel.

A. Fattah
Industrial Production Engineering Department., Faculty of Engineering., El-Mansoura University., Mansoura., Egypt.

E. Mokhtar
Production Engineering Department., Faculty of Engineering., El-Menia University., Minia., Egypt.

Recommended Citation

Fattah, A. and Mokhtar, E. (2021) "Influence of Elevated Temperature on Fracture Behavior of Stainless Steel.," *Mansoura Engineering Journal*: Vol. 25 : Iss. 3 , Article 8.
Available at: https://doi.org/10.21608/bfemu.2021.146695

Mansoura Engineering Journal, (MEJ), Vol. 25, No. 3, September 2000. M. 14

INFLUENCE OF ELEVATED TEMPERATURE ON FRACTURE BEHAVIOR OF STAINLESS STEEL

دراسة تأثير درجات الحرارة المرتفعة على أداء وسلوك الكسر لسبيكة الصلب الأوستنيتي

A.A.FATTAH* and E.MOUKHTAR**

خلاصة:

نظرا لأهمية المبادلات الحرارية المستخدمة في محطات تصنيع الأسمدة فقد عنى هذا البحث بتطبيق معايير علم ميكانيكا الكسور في دراسة سلوك الكسر لسبيكة الصلب الأوستنيتي 316 المستخدم في تصنيع أنابيب التبادل الحراري لهذه المحطات وقياس مدى مقاومة هذه السبيكة لنمو الشروخ تحت تأثير الأحمال الميكانيكية التي تسبب حالات إجهاد الزحف والزحف المصاحب للكلل بالإضافة إلى إجهاد الكلل المباشر عند تعرضها لدرجات الحرارة العالية. وقد أجريت تجارب معملية باستخدام عينات قياسية مصنعة من سبيكة الصلب الأوستنيتي 316 شكلت في منتصفها حزوز على شكل حرف V لتحفيز نمو الشروخ تحت تأثير الإجهادات المختلفة ودرجات الحرارة المرتفعة. وقد أهتم البحث بإجراء تجارب على عينات مماثلة في الشكل والأبعاد مصنعة من سبيكة الصلب الأوستنيتي 304 لعقد دراسة مقارنة بين المعدنين عن مدى مقاومة كلا المعدنين لمعدل نمو الشروخ تحت تأثير نفس الإجهادات التجريبية عند ارتفاع درجات الحرارة إلى مستويات حرارية تقدر بنسبة من درجة حرارة انصهار المعدن الأوستنيتي المصنع منه العينات في نطاق يتراوح بين درجة حرارة الغرفة وحتى حوالي 0.5 من درجة حرارة انصهار المعدن.

ونظرا لعدم وجود صيغة تجريبية مباشرة لقياس مدى مقاومة هذا المعدن لمعدل نمو الشروخ فقد اقترح في هذا البحث صيغة تجريبية مبسطة مستنتجة بالتوافق مع نتائج التجارب المعملية أمكن استخدامها في حساب وتقدير معدلات نمو الشروخ لسبيكة الصلب الأوستنيتي316 تحت تأثير الزحف وإجهاد الكلل والتأثير التبادلي لكل منهما عند تعرض العينة لدرجات الحرارة المرتفعة.

وخلص تحليل النتائج إلى توافق نتائج التجارب المعملية مع نتائج المعادلات التجريبية المقترحة المقدمة في هذا البحث مما يتيح طريقة سهلة ومبسطة لدراسة سلوك المكونات الهندسية عند تعرضها لحالات الإجهادات الميكانيكية تحت تأثير درجات الحرارة المختلفة باختلاف ظروف التشغيل.

وأشارت نتائج الفحص الكيميائي ومقارنة الخواص الميكانيكية لكلا السبيكتين إلى ضرورة موازنة العناصر المعدنية المضافة مثل موازنة عنصر النيكل المضاف إلى سبيكة الصلب الأوستنيتي المصنع منه أنابيب المبادلات الحرارية بما يسمح برفع مقدار معامل الإطاقة الحرجة لمقاومة المعدن لمعدل نمو الشروخ وهو ما أكدته مقارنة النتائج المعملية وكذلك نتائج الصيغة التجريبية المقترحة في هذه الدراسة من تميز سبيكة الصلب الأوستنيتي 304 من ارتفاع معامل الإطاقة وارتفاع مقاومة سبيكة هذا المعدن لمعدل نمو الشروخ عن سبيكة الصلب الأوستنيتي316 تحت تأثير إجهاد الكلل عند تعرض المعدن للدرجات الحرارة المرتفعة.

ABSTRACT

Fracture mechanics approaches have been employed to study the fracture behavior of the exchanger tubes made of austenitic stainless steel at elevated temperatures in fertilizer plant. Test conditions range from ambient to elevated temperature, monotonic to cyclic loading, and creep. Experimental work was carried out for creep, creep-fatigue interaction and fatigue at ambient and high temperatures on notched specimens. The temperature test was grouped into the range of homologous temperature (T/T_m) in the range of 0.177 (RT), 0.3, 0.40 and 0.50 of melting point for AISI 316 stainless steel. Furthermore experimental work has been extended, by using another group of specimens made of AISI 304 stainless steel. Chemical composition analysis and tensile tests were initially performed to record the mechanical properties of both materials at room temperature

Parametric representation of crack growth rate in terms of independent variables in Region II of crack growth curves has been proposed for creep, creep-fatigue interaction and fatigue of 316 stainless steel at ambient and high temperature rates. To demonstrate the validity of the present approach, the proposed equation has been used to

* Industrial Production Engineering Dept, Faculty of Engineering, Mansoura University, EGYPT.

** Production Engineering Dept, Faculty of Engineering, EL-Menia University, EGYPT

Accepted September 23, 2000

determine the fatigue crack growth rate versus the change in the stress-intensity-factor relationship for AISI 304 stainless steel.

Based on this study, experimental results as well as analytical results obtained by using the proposed equation for AISI 316 and AISI 304 stainless steel were analyzed, and recommendations for applications are made. Thus in the present study it has been attempted to obtain a simple criterion for crack growth behavior in AISI 316 stainless steel under high temperature creep, fatigue and creep-fatigue interaction conditions.

KEY WORDS

Creep, fatigue; creep-fatigue interaction, crack growth rate; stress intensity factor, homologous temperatures, notched specimen, austenitic stainless steel.

INTRODUCTION

Austenitic stainless steels, used over a wide temperature range, are often employed in components, which are loaded under severe conditions [1-4]. Microcracks can occur where stress concentrations exist at notches and welds. Growth and linkage of these microcracks result in the formation of a large crack whose propagation is influenced by such effects as the load fluctuations, cyclic loading, frequency, load waveform and thermal cycling value etc. [5-7]. This phenomenon involves the growth of small defects into macro or micro cracks that grow until fracture toughness of the components material is exceeded and catastrophic failure occurs [8-10]. In order to predict component lives, a complete understanding is needed of the behavior of material under creep, fatigue and creep-fatigue interaction [11-15].

The current study is concerned with crack growth of AISI 316 stainless steel subjected to cyclic loading conditions at high temperature since propagation is the dominant process of short life fatigue of structural component. It is also concerned with proposition of an empirical expression to provide a simple criterion for crack growth behavior under high temperature.

EMPIRICAL APPROACH

In consideration of the controlled load, loading have been represented as shown in Fig 1(a), (b) and (c) for creep-fatigue interaction, creep and fatigue respectively. Parametric representation of crack growth in Region II of crack growth curve for cyclic loading conditions at ambient and high temperature ratios is proposed as given in the following.

I-Representation of crack growth rate in terms of independent variables is proposed for creep, creep-fatigue interaction and fatigue at ambient and high tetoperatures, respectively. However, based on PARIS equation [16], the proposed equation is expressed by the following empirical relationship:

$$\frac{da}{dt} = A_{Nt}\, B_{fc} \cdot \sigma_c^m . \Delta K_I^n \; . \exp - \left(\left(\frac{f_K}{f_T} \right) - f_{Ht} \right)$$

$$\frac{da}{dN} = B_{fc} \cdot \sigma_c^m . \Delta K_I^n \; . \exp - \left(\left(\frac{f_K}{f_T} \right) - f_{Ht} \right) \qquad (1)$$

where K_I is the opening mode-stress intensity factor, σ_c is the applied stress, m, n, A_{Nt} and B_{fc} all are constants.

These constants were estimated by the best fit through the data obtained from the experimental work performed using the test specimen made of type AISI 316 stainless steel. In addition, A_{Nt} is a constant depending on the fatigue test number of cycle, and B_{fc} is a constant which has been suggested to be related to the obtained tensile mechanical properties ($\sigma_{0.2\%}$ the 0.2% proof stress, σ_{ult} the tensile strength and E the material modulus of elasticity of the specimen material at room temperature). However, B_{fc} would be computed by using the following form:

$B_{fc} = (\sigma_{0.2} + \sigma_{ult})/E$

In the proposed equation (1), high temperature, holding time and stress rapture factors f_T, f_{Ht} and f_K have been suggested by a function of the form:

$f_T\{\varphi(T,T_m)\} = [T/T_m]$

$f_{Ht}\{\psi(t_H,t_c)\} = t_c/(t_H+t_c)$

$f_K\{\Phi(K_{Ii},K_{If})\} = [1-(\sigma_i/\sigma_f)\sqrt{(a_i/a_f)}]$

where a_i is the initial crack length, a_f is the crack length at fracture, σ_i is the true stress at the start of Region II, σ_f is the applied stress at fracture, t_H is holding time, t_c is fatigue frequency time per cycle and T/T_m is homologous temperature.

The interchanging factor A_{Nt} controls the relation between da/dN and da/dt as follows:

$$\frac{da}{dN} = \frac{1}{A_{Nt}} \cdot \frac{da}{dt}$$

$A_{Nt} = N.(R_d)$

where $R_d = N_s/N_o$ is the frequency reduction ratio, N_o is the number of rotation per minute of driving motor shaft and N_s is the selected number of rotating per minute of cam eccentric shaft.

The stress intensity factor K_I for round bars is expressed by [17] as follows:

$$K_I = (\pi . a)^{1/2} . \sigma . f\left(\frac{2a}{d_c}\right) \quad (2)$$

where $f\left(\frac{2a}{d_c}\right) = 1 + 3\left(\frac{2a}{d_c}\right) + 3\left(\frac{2a}{d_c}\right)^2 + \left(\frac{2a}{d_c}\right)^3$

Thus, in accordance with the proposed equation (1), high temperature crack growth rate under creep, fatigue and creep-fatigue interaction may be expressed by the following relationships:

A-For creep

$$\frac{da}{dt} = A_{Nt} . B_c . \sigma_c^m . \exp-\left(\left(\frac{f_K}{f_T}\right) - f_{Ht}\right) \quad (3)$$

$B_c = (\sigma_{uk}/E)$

B-For creep-fatigue interaction

$$\frac{da}{dN} = .B_{fc} . \sigma_c^m . \Delta K_f^n \ . \exp-\left(\left(\frac{f_K}{f_T}\right) - f_{Ht}\right) \quad (4)$$

$B_{fc} = (\sigma_{0.2}+\sigma_{uk})/E$

C-For fatigue

$$\frac{da}{dN} = B_f . \Delta K_f^n \ . \exp-\left(\left(\frac{f_K}{f_T}\right) - f_{Ht}\right) \quad (5)$$

$B_f = (\sigma_{0.2}/E)$

II-Representation of the propagation life (number of cycles to failure for crack propagation) in region II can be expressed as following.

$$N_f = \frac{1}{A . Y^m . \Delta\sigma^m .}\left(\frac{2}{m-2}\right)\left[\frac{1}{a_i^{\frac{m-2}{2}}} - \frac{1}{a_f^{\frac{m-2}{2}}}\right] \quad (6)$$

where N_f is the number of cycles to failure, $\Delta\sigma$ is the stress range and Y is the geometrical correction factor.

EXPERIMENTAL WORK

Chemical composition inspection and tensile test was initially performed to record the material chemical composition and the mechanical properties of both AISI 316 as well as AISI 304 stainless steel at room temperature. The specimens employed in tensile test were the ASTM standard 25,4 mm gage length. Fatigue specimens were then machined into the shape and required dimension (AISI SS samples do=6.35mm, dc=5.35mm. and 2a=1mm) according to ASTM code as shown in Fig. 2. Chemical composition and Mechanical properties at room temperature of this AISI 316 stainless steel is shown in Table 1 and Table 2 respectively.

TABLE 1. Chemical Composition (wt %) of AISI 316 stainless steel.

Material	C	Ni	Cr	Mo	Mn	Si	P	S
AISI 316	0.05	10.95	16.9	2.12	1.46	0.42	0.036	0.022

TABLE 2. Mechanical Properties for AISI 316 stainless steel at RT.

Yield Stress MPa.	Tensile Strength MPa.	Elongation %	Reduction of Area %	Hardness Hv
275	630	60	71	157

Tests of creep, creep-fatigue interaction and fatigue at different temperature levels, representing 0.177 (RT), 0.35, 0.40, 0.45 and 0.50 of melting point of the tested material were performed under load control condition. Experimental work has been extended, by using another group of specimens made of AISI 304 stainless steel. The chemical composition and the mechanical properties at room temperature of AISI 304 stainless steel are given in Tables 3 and 4, respectively.

TABLE 3. Chemical Composition (wt %) of AISI 304 stainless steel.

Material	C	Ni	Cr	Mo	Mn	Si	P	S
AISI 304	0.06	8.85	18.12	0.11	1.12	0.58	0.028	0.006

TABLE 4. Mechanical Properties for AISI 304 stainless steel at R T.

Yield Stress MPa.	Tensile Strength MPa.	Elongation %	Reduction of Area %	Hardness Hv
330	650	47	56	159

Experiments were carried-out using a specially designed mechanical apparatus equipped with a special cam system and load control mechanism. Schematic representation of the testing apparatus is shown in Fig. 3. Each end of the specimen is screwed into the specimen holders. The optical technique is adapted to measurements on the tested specimens, since the crack length can be estimated relative to the notch opening displacement. Crack detection and the measurement of notch opening displacement was made during running the testes by using a microscope through a peeping window with 100X magnification. A specially fabricated circular chamber provided with helical resistance heater was used to heat the specimen to the required temperature. Specimen temperatures were continuously monitored with thermocouple that was fixed to the specimen in vicinity of the specimen notch. The load waves were controlled for creep, fatigue and creep-fatigue interaction by adjusting the eccentric stroke. Thus, by changing the holding time t_H, the loading wave (Fig. 1a) which is the combination of the creep loading wave (Fig. 1b) and the fatigue loading wave (Fig. 1c) can be obtained. Cyclic load is applied by means of a lever and rotating cam system. The frequency of the fatigue-loading wave was 60 cpm, and the waveform was sinusoidal. Crack initiation under loading conditions at σ_{app} = 189 MPa. The values of the applied stress σ_{app} corresponding to the maximum tensile stress were ranged between 130-210 MPa. The FCG rates (da/dN) were determined by dividing each increment of crack extension by number of cycles producing that increment.

On all specimens, the circumferential notch was V-shaped with 30° angle. After notching the specimen with a lathe tool, the notch root radius obtained in the specimen was further reduced with a razor blade which were mounted on the tool post of the lathe through a specially fabricated fixture. The use of the razor blade produced a very sharp notch tip radius, $\rho \approx 0.05$ mm.

DISCUSSION

The most frequently used correlation between FCG rate and the stress intensity factor is the power low proposed by Paris (1963) [16]:

$da/dN = C\,\Delta K^m$

where C and m are material constants.

Paris equation predicts a linear relationship between log (da/dN) and log (ΔK), but it holds only for intermediate FCG region under normal temperature condition.

Several investigations have been conducted to study the effect of stress ratio ($R=K_{max}/K_{min}$) for variable loading at normal temperature condition on fatigue crack propagation rate. Barsom, [18] has proposed the following form:

$da/dN = A\,(\Delta K)^m / \sqrt{(1-R)}$

where the stress ratio $R \geq 0$.

Solomon and Coffin (1973) [19] pointed-out that, crack growth rate was seen to increase with decrease in frequency and they expressed the following empirical relationship for elevated temperature:

$da/dN = C\,(\Delta K)^\alpha\, f^\beta$

where ΔK is the stress intensity factor range, f is the frequency, C., α and β are material constant, and γ were temperature and material constants.

This type of relationship has been used by Yokobori and Sato (1976) [20] at room temperature.

Based on Solomon equation, Plumtree and Schafer (1984) [21] have developed the following expression:

$da/dN = C\,(\Delta K)^\alpha\, f^\beta\, \delta^\gamma$

where δ is the ratio of loading to unloading times.

Based on another line of considerations, the present work proposes a more general equation that takes into consideration the effects of high temperature rates, holding time and stress rapture factors f_T, f_H and f_K. However, parametric representation of high temperature crack growth rate in terms of independent variables, such as K, σ_{app}, temperature effect and some material constants have been suggested as given in equation (1). The values of *m*, *n*, and B_{fc} were suggested in this work in accordance with creep, creep-fatigue interaction and fatigue loading conditions for type AISI 316 stainless steel.

The present results show m= 3.1 for creep, m=1 and n=3.21 for creep-fatigue interaction and n=3.63 for fatigue loading conditions respectively to correl te for AISI 316 stainless steel at room temperature. A line fit regression was used to obtain the best fit through the experimental data resulted from the tests that performed at ambient and high temperature rates. The results given in Table 5. show the best-fit representation of the constants for equations 3,4 and 5.

TABLE 5.Constants of equations 3,4 and 5 by best-fit representation for type AISI 316 stainless steel.

Loading condition	M	N	B_{fc}	t_H sec	σ_{app} MPa
Creep equ. (3)	3.1	0	3.15×10^{-3}	∞	130-210
Creep-fatigue interaction equ.(4)	1	3.21	4.525×10^{-3}	60	189
Fatigue equ. (5)	0	3.63	1.375×10^{-3}	0	189

To satisfy the physical reality that unstable crack growth occurs rapidly when the operating temperature approaches a high temperature rates, the effective empirical factor f_K, f_H and f_T for equations 3,4 and 5, have been taken into account.

In consideration of the possibility of creep, creep-fatigue interaction and fatigue effect, on notched specimen at different temperature rate, tests were conducted and results are plotted as shown in Figures 4-12.

The crack tip radius upon the specimens or component performance can be indicated by the fatigue life for notched specimens as represented by the curves shown in Fig 4. It's evident that the specimen having sharper crack tip is the shorter fatigue life. Thus, the presence of notch, crack decreases the material creep and fatigue resistance.

The curves shown in Fig. 5, indicate that, at normal as well as elevated temperature, the notched specimen will develop cracks. Further, when a crack has grown at high temperature, the stress intensity factor K_I come closer the critical value K_c and the crack accelerates more rapidly until the critical stress intensity factor K_C is exceeded and final catastrophic failure occurs.

To demonstrate the validity of equations 3,4 and 5, the values of the m, n and B_{fc} as given in table 5 for AISI 316 stainless steel have been used to determine the relationship of da/dN versus ΔK (see appendix-A).

The proposed equations 3,4 and 5 have been employed to develop a family of curves representing the relationship between da/dN versus ΔK as shown in Figures 6-10 for AISI 316 stainless steel under creep, creep-fatigue interaction and fatigue loading conditions ambient and high temperature rates.

Analyzing the resulted curves shown in these figures indicate that, the reduction in fatigue life at elevated temperature was mainly due to the presence of cracks that grown at the tip of the notch rather than the creep-fatigue effects. .In addition the time dependent deformation as with all deformation processes, is largely dependent upon the chemical composition as well as the mechanical properties of the material. Therefore, the development of alloys with a high resistance to creep-fatigue at elevated temperature involves producing a material in which movements of dislocations only take place with difficulty. However to verify this statement it has been intended to extend the experimental work by using another group of specimens made of AISI 304 stainless steel.

Comparison of the results shown in Figs, 11and 12, indicate that, there is an improvement in the creep-fatigue metal resistance for the AISI 304 stainless steel at elevated temperature higher than that for AISI 316 stainless steel. However, it's evident that this improvement in the creep-fatigue resistance is attributed to the addition of elements whose atomic size and valence are largely different from basic material such as chromium. In addition, it is recommended to increase the critical crack size at failure by using a material with a higher fracture toughness stress such as AISI 304 stainless steel (K_{IC} value is 117 MPa.$\sqrt{m}$ for 304 and is 98 MPa.$\sqrt{m}$ for 316 stainless steel).

Ultimately, it is clearly visible that material which is susceptible to creep-fatigue effects at elevated temperatures should only be subjected to stresses which keep it in the secondary region of straight-line through its service life.

CONCLUSIONS

Creep, fatigue and creep-fatigue interaction tests were performed at different temperature rates that are related to the material melting point on AISI 316 stainless steel specimens machined with V-notches. In addition, the experimental work has been extended, by using some specimens made of AISI 304 stainless steel.
An empirical expression to provide a simple criterion for crack growth behaviors under high temperature from the practical point of view has been developed.

1-An extensive program of creep, creep-fatigue interaction and fatigue tests has been carried out on type AISI 316 stainless steel over the homologous temperature range 0.177-0.5.

2-A parametric representation formula of high temperature crack growth rate in terms of independent variables and some material constants taken into consideration the effects of high temperature rates, holding time and stress rapture factors has been proposed in this work.

3-A line fit regression was used to obtain the best fit through the experimental data, and evaluate the effective empirical factors

4-The developed equation successfully modeled the crack propagation rate versus stress-intensity-factor range and a family of temperature dependent curves have been derived under creep, creep-fatigue interaction and fatigue loading conditions for type AISI 316 stainless steel over the homologous temperature range 0.177-0.5.

5-The derived curves are expected to be applicable to the AISI 316 stainless steel as well as AISI 304 stainless steel. Therefore, proposed approach is believed to be simpler than those currently published in the available literatures.

6-Comparison between the analyzed results on type AISI 316 stainless steel and type AISI 304 stainless indicated that the creep-fatigue-resisting alloy is further strengthened by added alloying elements such as chromium, but this limits the amount that may be added. Thus, the use of alloying elements that raise the creep-fatigue metal resistance at elevated temperature will be beneficial.

ACKNOWLEDGMENT

The author extends his sincere thanks to Engineer T. Salama Head of Plant Sectors and Vice President of Delta Semad Company, Talkha, Mansoura, EGYPT for conducting the cyclic tests.

REFERENCES

1-SADANANADA, K., and SHAHINIAN, P., "Effect of environment on crack growth behavior in Austenitic stainless steel under creep and fatigue conditions" Metallurgical Transactions A, 11A, p 267-276 (1980).

2-MASS, E., and PINEAU, A., "Creep crack initiation and growth in an austenitic stainless steel" Proc. of the fourth international Conf. on Mechanical Behavior of Materials, STOCKHOLM, SWEDEN, p783-770 (1983).

3-ATANASIU, N., E., and IRIMESCU, B., R., "Fatigue crack propagation and threshold of type 304L austenitic stainless steel" Proc. of the fourth international Conf. on Mechanical Behavior of Materials, STOCKHOLM, SWEDEN, p841-848 (1983).

4-MAJUMDAR, B., S., ASKE, C., E., and MANHAN, M., P., "Creep crack growth characterization of type 316 stainless steel using miniature specimens" Int. J. of Fracture vol. 47 p127-144, (1991).

5-SONG, S., H., KANG, M., S., and KIM, K., Y., "Low cycle fatigue crack propagation behavior of 1.5Cr-0.7Mo steel at high temperature" Proc. of Conf. on fatigue, AUSTRALIA, p1613-1620 (1997).

6- 7-BERGER, G., and WIEMANN, W., "Effect of tension compressive cycling on fatigue crack growth" Proc. of ICF-6, Advances in Fracture Research, p1799-1806 (1984).

7-HSU, C., H., "The fatigue cracking of titanium tubes in an industrial heat exchanger" Fatigue Life: Analysis and Prediction, Proc. of the international Conference on Fatigue, Corrosion Cracking, Fracture Mechanics and Failure Analysis, Salt Lake City, USA, p79-82 (1985).

8-ZHAN, G., D., and REECE, M., J., "Fatigue growth behavior of short cracks" Proc. of Conf. on fatigue, AUSTRALIA, p1677-1684 (1997).

9-OBABUEKI, A., M., A., LEE, C., TANAKA, T., and LEE, S., "A unified model for fatigue crack initiation and growth, with emphasis on short-crack closure effects, variable temperature fatigue and creep-fatigue interaction" J. Material Science and Engineering A103, p71-93 (1988).

10-STEEN, M., PROVOST, W., and DHOOGE, A., "An internal variable approach to creep-fatigue and their interaction at elevated temperature" Proc. of ICF-6, Advances in Fracture Research, p2273-2280 (1984).

11-HAMEL, F., G., THERIAULT, G., and MASOUNAVE, J., "A simple procedure for prediction of fatigue crack growth rate under variable amplitude loading" Fatigue Life: Analysis and Prediction, Proc. of the international Conference on Fatigue, Corrosion Cracking, Fracture Mechanics and Failure Analysis, Salt Lake City, USA, p275-282 (1985).

12-GUOZHI, LU, "Fatigue crack closure study during fatigue test" Fatigue Life: Analysis and Prediction, Proc. of the international Conference on Fatigue, Corrosion Cracking, Fracture Mechanics and Failure Analysis, Salt Lake City, USA, p143-146 (1985).

13-LIOYD, G.J. and wareing, J., "Life prediction method for combined creep-fatigue" Metals Technology, pp.295-305, (1981).

14-SMITH, D., J., and ELLISO, E., G., "Modeling crack growth for creep and fatigue loading" Int. J. Pres. Ves. and Piping Vol. 50, p231-241 (1992).

15-MONKMAN, F.C., and Grant, N.H., "An empirical relation between rupture life and minimum creep rate in creep rupture tests" Proc. ASTM 56, 593 (1956).

16-PARIS, P., C., "The fracture mechanics approach to fatigue" An interdisciplinary approach, Syracuse University Press., SYRACUSE, NY, p107-132 (1963).

17-FATTAH, A. A. "Fracture studies and a procedure for K_{ISC} determination to control and prevent failure of rotating shafts" Mansoura Engineering Journal (MEJ) vol. 22, No. 1., 1-13, (1997).

18-BARSOM, J. M., "Fatigue crack growth under variable amplitude loading in ASTM A514 steel" ASTM STP 536, American Society for Testing and Materials, Philadelphia, (1973).

19-SOLOMON, H. D., COFFIN, L. F., "Effects of frequency and environments on fatigue crack growth" Fatigue at elevated temperatures, STP 520, ASTM, Philadelphia, p112-122, (1973)

20-YOKOBORI, T., and SATO, K., "The effect of frequency on fatigue crack propagation rate" J. Engineering Fracture Mechanics vo., 8 p81-88 (1976).
21-PLUMTREE, A. and SCHAFER, S., "Waveform and frequency effects on the high temperature fatigue crack propagation rate of stainless steel" Proc. of ICF-6, Advances in Fracture Research, p2249-2256 (1984).

Appendix-A

Parametric representation of crack growth rate for AISI 316 stainless steel

Based on PARIS equation [16], the proposed equation is expressed by the follows:

$$\frac{da}{dt} = A_{Nt} B_{fc} . \sigma_c^m . \Delta K_I^n \ . \exp-\left(\left(\frac{f_K}{f_T}\right) - f_{Ht}\right)$$

$$\frac{da}{dN} = B_{fc} . \sigma_c^m . \Delta K_I^n \ . \exp-\left(\left(\frac{f_K}{f_T}\right) - f_{Ht}\right) \qquad \text{(i)}$$

To demonstrate the validity of equations (I), thus the crack growth rate for AISI 316 stainless steel specimens ($\sigma_{0.2\%}$=275 MPa. $\sigma_{ult.}$=630 MPa. E=2.x 10^5 MPa. and K_c=98 MPa.√m., at room temperature) under creep, creep-fatigue interaction and fatigue loading conditions at different temperature ratio would be determined as follows:

A-Creep:

$B_c = (\sigma_{ult.}/E) = 3.15\times10^{-3}$

$A_{Nt} = N.R_{d} = 1500\ (1/25) = 60$ cpm.

where A_{NT} is corresponding to test frequency f (test number of cycles per minute).

$t_c = 1/f = 4.3\times10^{-2}$ $\qquad$ $t_H = \infty$ sec $\qquad$ $f_{Ht} = t_c/(t_H+t_c) \approx 0$

where the homologous temperature factor f_T is varying between 0.177 t0 0.5 (298 to 842 K° in respect to AISI 316 austenitic stainless steel milting point of 1684 K°).

Substituting the values of A_{Nt}, B_c, m, n, f_K, f_T and f_{Ht} into equation (3) gives

$$\frac{da}{dt} = (60/60)\times 3.15\times10^{-3} . \sigma_c^{3.1} . \exp-\left(\frac{f_K}{f_T}\right)(\mu m/s) \qquad \text{(ii)}$$

where m=3.1 and n=0

$\Delta\sigma = \Delta K / f(2a/d_c) . \sqrt{\pi a}$.

$f_K = (K_{If} - K_{Ic}/K_{If})$

$= [1 - (\sigma_i/\sigma_c)\sqrt{(a_i/a_f)}]$

B-Creep-Fatigue interaction:

$B_{fc} = (\sigma_{0.2\%} + \sigma_{ult.})/E = 4.525\times10^{-3}$

$t_c = 4.3\times10^{-2}$ $\qquad$ $t_H = 60$ sec. $\qquad$ $f_{Ht} = 7.14\times10^{-4}$

Substituting the values of B_{fc}, f_K, f_T and f_{Ht} that correspond to the creep loading condition into equation (4) gives

$$\frac{da}{dN} = 4.525\times10^{-3} . \sigma_c . \Delta K_I^{3.21} \ . \exp-\left(\left(\frac{f_K}{f_T}\right) - f_{Ht}\right)(\mu m/cycle) \qquad \text{(iii)}$$

where m=1 and n=3.21.

C-Fatigue:

$B_f = (\sigma_{0.2\%}/E) = 1.375\times10^{-3}$

$t_H = 0$ sec. $\qquad$ $f_{Ht} = 1$

Substituting the values of B_f, f_K, f_T and f_{Ht} that correspond the creep loading condition into equation (5) gives:

$$\frac{da}{dN} = 1.375\times10^{-3} . \Delta K_I^{3.63} . \exp-\left(\left(\frac{f_K}{f_T}\right) - 1\right) (\mu m/cycle) \qquad \text{(iv)}$$

where m=0 and n=3.63.

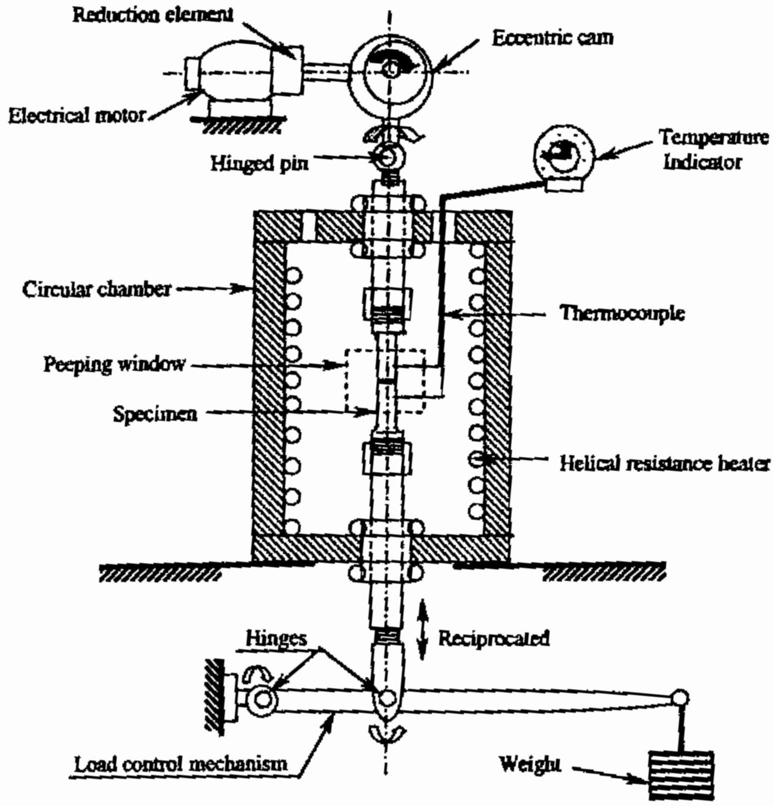

Fig. 3. A schematic diagram for a typical creep-fatigue testing apparatus.

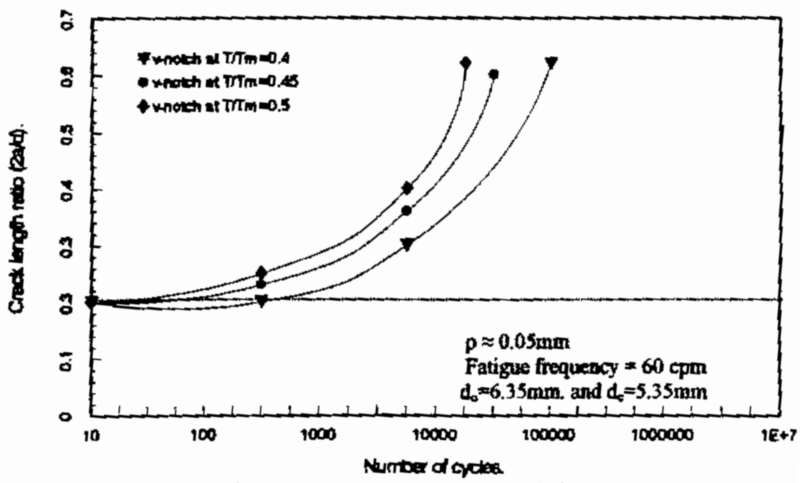

Fig. 4. Effect of high temperature rates on the fatigue crack growth as a function of number of cycles to failure, for 316 stainless steel.

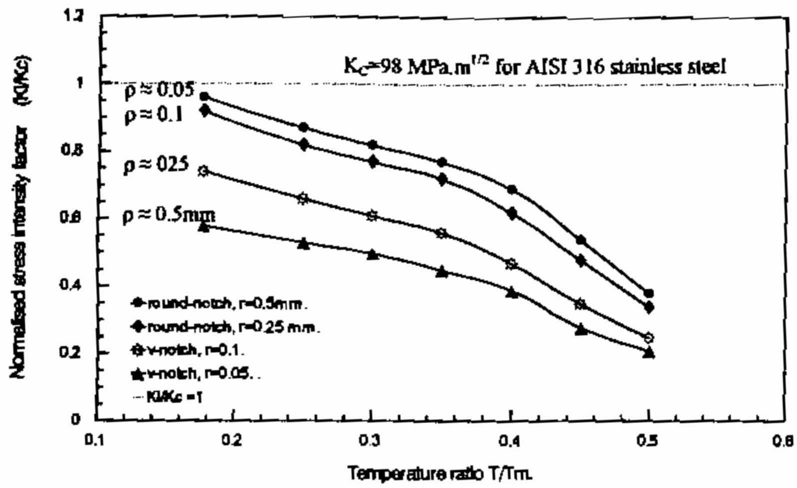

Fig. 5. Effect of crack tip radius on the normalized stress-.ntensity factor at different temperature ratio, for 316 stainless steel.

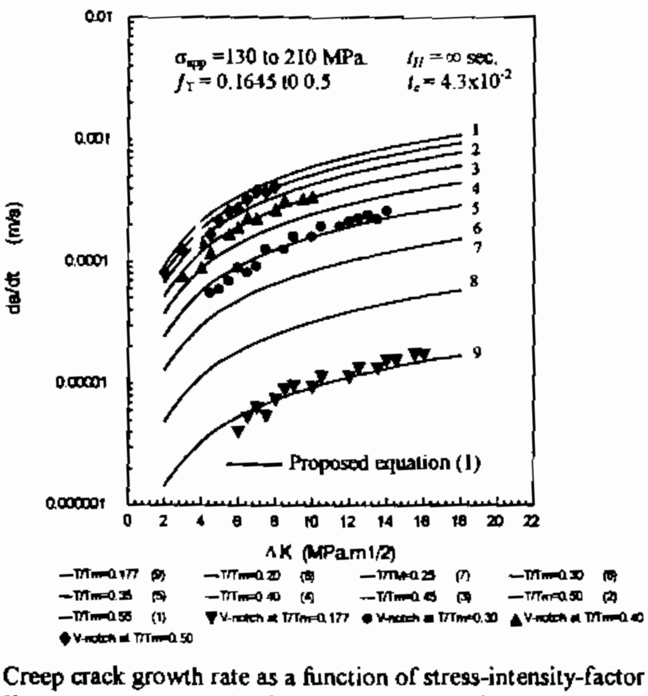

Fig. 6. Creep crack growth rate as a function of stress-intensity-factor at different temperature ratio, for 316 stainless steel ($\rho \approx 0.05$mm).

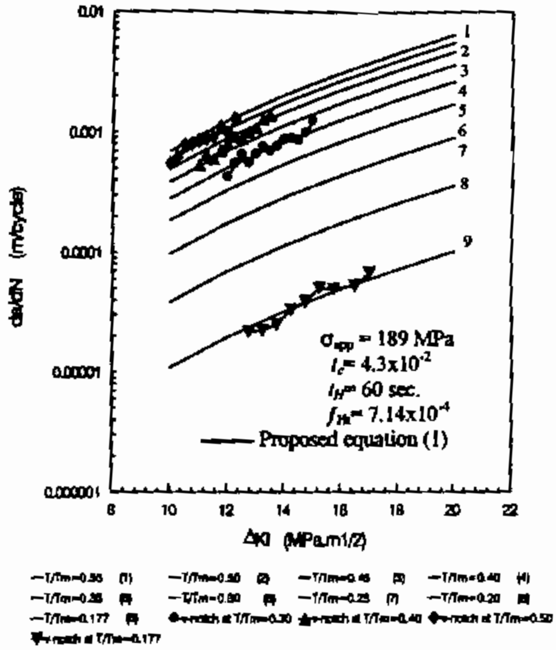

Fig. 7. Creep-Fatigue interaction crack growth as a function of stress-intensity-Factor at different temperature ratio, for 316 stainless steel (ρ ≈ 0.05mm).

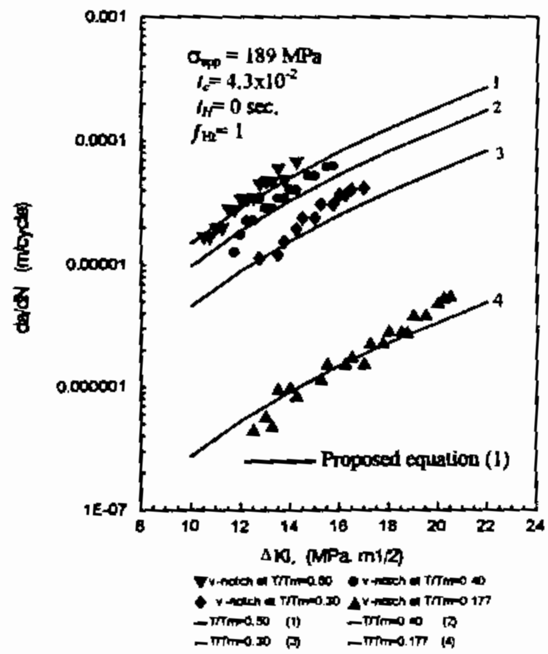

Fig. 8. Fatigue crack growth as a function of stress-intensity-factor at different temperature ratio for316 stainless steel (ρ ≈ 0.05mm).

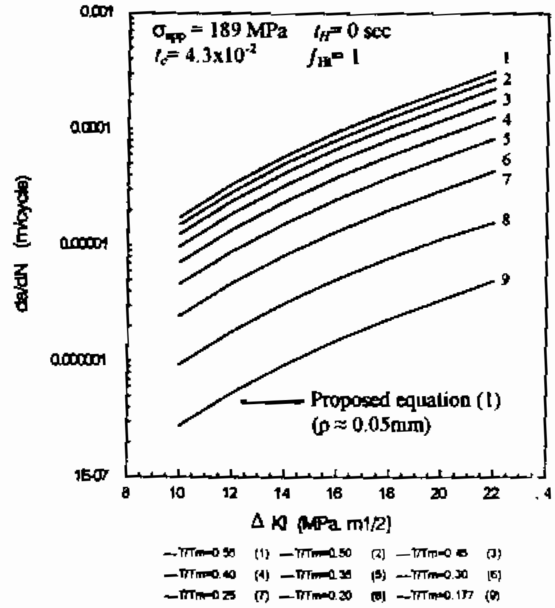

Fig.9, Effect of homologous temperature ratio (T/T_m) on crack growth ratio *da/dN* vs. stress intensity factor (ΔK_I) for 316 stainless steel using the proposed equation.

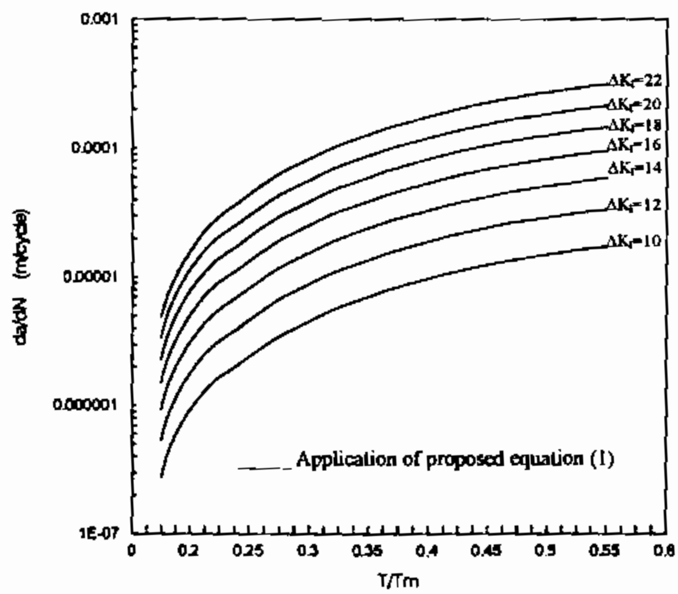

Fig. 10, Effects of T/T_m on the fatigue crack growth rates *(da/dN)* at different value of stress-intensity-factor (ΔK_I) for 316 stainless steel using the proposed equation (1).

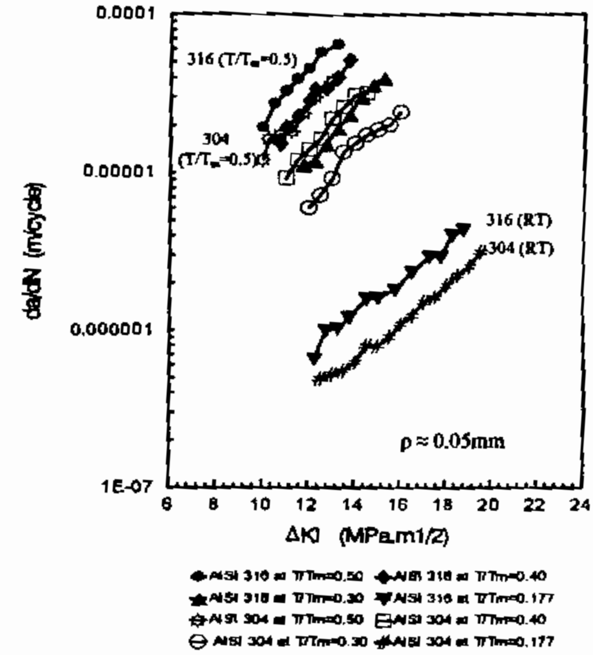

Fig. 11. Comparison of experimental crack growth rate vs. stress-intensity-factor range for AISI 316 and AISI 304 (Experimental results).

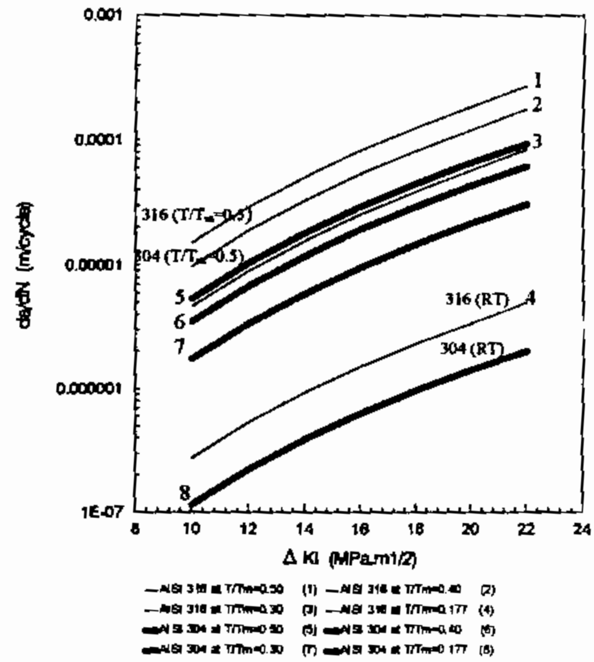

Fig. 12. Comparison of analytical crack growth rate vs. stress-intensity-factor range for AISI 316 and AISI 304 using the proposed equation (1).